RAPID COMMUNICATIONS

PHYSICAL REVIEW B VOLUME 40, NUMBER 4 1 AUGUST 1989

Electron-phonon coupling in superconducting $Ba_{0.6}K_{0.4}BiO_3$: A Raman scattering study

K. F. McCarty
Sandia National Laboratories, Livermore, California 94551

H. B. Radousky
Lawrence Livermore National Laboratory, Livermore, California 94550

D. G. Hinks, Y. Zheng, and A. W. Mitchell
Argonne National Laboratory, Argonne, Illinois 60439

T. J. Folkerts and R. N. Shelton
Department of Physics, University of California–Davis, Davis, California 95616
(Received 20 March 1989)

Superconducting and nonsuperconducting phases in the $Ba_{1-x}K_xBiO_3$ system have been studied at temperatures down to 4 K by use of Raman spectroscopy. For superconducting $Ba_{0.6}K_{0.4}BiO_3$, an optical phonon at 348 cm^{-1} (43 meV) has the distinctive Fano line shape indicative of significant coupling between the phonon and a broad electronic continuum. For nonsuperconducting $Ba_{0.8}K_{0.2}BiO_3$, the same phonon is not observed to be coupled to the electronic states. Assignment of the 348-cm^{-1} peak to specific normal modes of vibration is discussed as is the similarity to the phonon at 340 cm^{-1} in $YBa_2Cu_3O_7$ that also exhibits electron-phonon coupling.

Within the framework of the new oxide superconductors, it is interesting to compare the Cu-based materials (La-Cu-O, Y-Ba-Cu-O, Bi-Ca-Sr-Cu-O, Tl-Ca-Ba-Cu-O, and their derivatives) with the Bi-based materials (Ba-K-Bi-O and Ba-Bi-Pb-O). While superconducting transition temperatures (T_c) approaching 125 K are found in the Cu-based materials,[1] T_c's of ~30 K have been found in the $Ba_{1-x}K_xBiO_3$ system.[2] In comparison to "conventional" superconductors, the T_c's of the $Ba_{1-x}K_xBiO_3$ system are still exceptional. In an effort to compare and contrast the nature of superconductivity in the Cu-based materials with the Bi-based materials, we have investigated the $Ba_{1-x}K_xBiO_3$ system using Raman spectroscopy. In order to explain the high T_c and the low density of electronic states at the Fermi level,[3] several approaches have been suggested in the literature. One approach involves coupling between electrons and high-frequency optical phonons[4,5] while other approaches rely on high-energy electronic excitations to mediate the superconductivity.[3]

Here we show that a high-frequency optical phonon is coupled to electronic states in superconducting $Ba_{0.6}K_{0.4}BiO_3$ (T_c = 24 K) but not in nonsuperconducting $Ba_{0.8}K_{0.2}BiO_3$. The Raman peak at 348 cm^{-1} (43 meV) that exhibits the distinctive Fano line shape as a result of the electron-phonon coupling is similar in frequency to the O vibration at ~340 cm^{-1} in $YBa_2Cu_3O_7$ that also exhibits electron-phonon coupling.[6]

Two sets of $Ba_{1-x}K_xBiO_3$ samples were prepared using two different synthesis techniques: low-density samples made by a sintering technique[7] and high-density samples made by a melt-processing technique.[8] Sintered (low-density) samples with x = 0.30, 0.35, 0.375, and 0.40 were prepared by mixing Bi_2O_3, KO_2, and BaO powders in a N_2 atmosphere in a glove bag. Since the initial purity of the BaO proved to be a crucial factor in determining sample quality, fresh batches of BaO were prepared from $BaCO_3$ powder prior to each preparation. The powders were first fired at 700 °C for 1 h in N_2, followed by 0.5 h in O_2 at 450 °C. Several refirings and regrindings were necessary to produce single-phase sintered samples (> 95%), as determined from powder x-ray diffraction. High-density samples (x = 0.20 and 0.40) were made by melting the oxide mixtures and rapidly cooling them in Cu molds. These materials were then fired in N_2 and O_2 as described above for the sintered samples. The superconducting samples all had an intense blue color. Magnetization curves obtained using a Quantum Design superconducting quantum interference device magnetometer are shown in Fig. 1. Onset of superconductivity in the sintered samples occurred at ~28 K with the x = 0.30 sample exhibiting only ~2% shielding. Onset in the high-density sample with x = 0.40 occurred at 24 K and an undistorted, cubic perovskite structure was established using neutron diffraction. The high-density sample with x = 0.20 showed contamination by unreacted $BaBiO_3$ and was not superconducting.

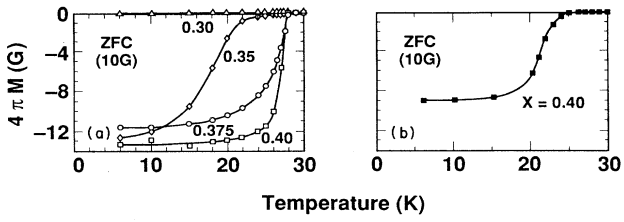

FIG. 1. Magnetization curves (zero-field cooled) for (a) sintered $Ba_{1-x}K_xBiO_3$ samples with x = 0.30, 0.35, 0.375, and 0.40; and (b) high-density sample with x = 0.40. No demagnetization factors have been applied to the data.

While the structures of the noncubic $Ba_{1-x}K_xBiO_3$ phases ($0 \leq x < 0.375$) are not known in great detail, neutron-diffraction results on the $x = 0.20$ phase indicate a $\sqrt{2}a \times \sqrt{2}a \times 2a$ supercell structure that is either orthorhombic or tetragonal.[9] In addition, an x-ray diffraction study has deduced a supercell structure with orthorhombic symmetry for $Ba_{0.96}K_{0.04}BiO_3$.[10]

Raman spectra were obtained in a backscattering geometry using the 488-nm line of an Ar-ion laser.[11] The high-density $Ba_{0.6}K_{0.4}BiO_3$ and $Ba_{0.8}K_{0.2}BiO_3$ samples were mounted on the cold finger of a liquid-helium refrigerator using grease. Temperatures were measured by an Fe-Au thermocouple mounted adjacent to the sample on the cold finger. Spectra in the refrigerator were obtained using 0.7 mW of power focused into a spot about 100 μm in diameter. Spectra of the sintered samples were taken at room temperature (RT) using about 5 mW of laser power.

Figure 2 illustrates the Raman spectra of the sintered $Ba_{1-x}K_xBiO_3$ samples with $x = 0.30$, 0.35, 0.375, and 0.40. All samples have a broad peak centered around 325 cm^{-1} and an extremely broad peak extending from about 375 to 650 cm^{-1}. Figure 3 illustrates the Raman spectra obtained from high-density $Ba_{0.6}K_{0.4}BiO_3$ between 295 and 4 K. For $x = 0.40$, the principal difference between the high-density and sintered samples is the greater intensity above ~ 375 cm^{-1} for the high-density sample. This feature has maximum intensity at 573 cm^{-1} and upon cooling, an additional peak at ~ 430 cm^{-1} develops. Several features are in common with results from superconducting $BaPb_{1-x}Bi_xO_3$,[12] most notably, both systems have Raman peaks near 325 cm^{-1}. For $Ba_{0.6}K_{0.4}BiO_3$, the evolution of the peak centered around 325 cm^{-1} with

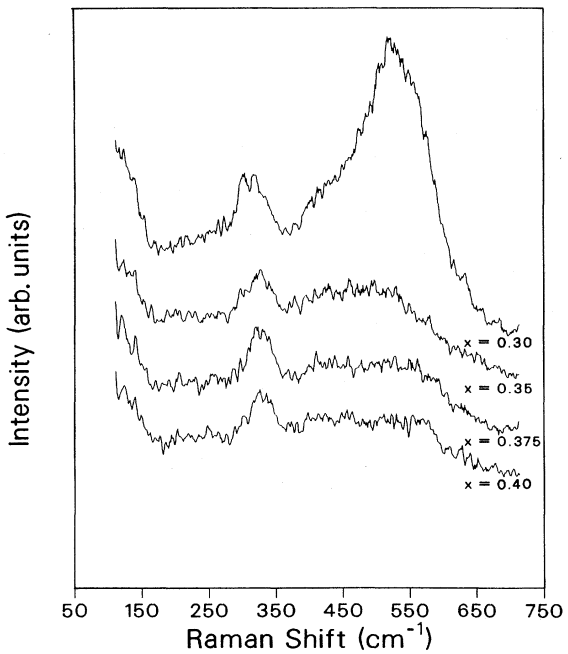

FIG. 2. Raman spectra of sintered samples of $Ba_{1-x}K_xBiO_3$ with $x = 0.30$, 0.35, 0.375, and 0.40 at RT. Absolute scaling of all spectra is the same with linear offsets for clarity.

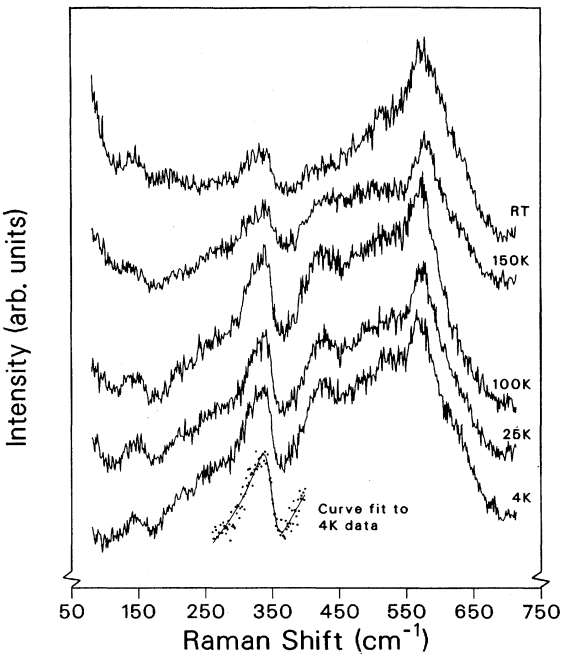

FIG. 3. Raman spectra of superconducting $Ba_{0.6}K_{0.4}BiO_3$ (high density, $T_c \approx 24$ K) between RT and 4 K. Absolute scaling of all spectra is the same with linear offsets for clarity. The partial spectrum shows the comparison between the least-squares fit to the Fano line shape (smooth curve) and the 4-K experimental data (solid circles).

temperature is most interesting (Fig. 3). Upon cooling below RT, the peak develops the distinctive Fano line shape,[13] i.e., the peak is highly asymmetric with the intensity dropping off sharply on the high-frequency side. Further, on the high-frequency side, the peak penetrates below the background which is increasing in intensity roughly linearly with increasing Raman shift. The Fano line shape occurs when scattering from an electronic continuum interferes with scattering from a discrete phonon.[13] Observation of a Fano line shape is persuasive evidence for strong coupling between the phonon and electronic states. The data of Fig. 3 were fit to the Fano line shape:[14]

$$I(\epsilon) = I_0 \frac{(q+\epsilon)^2}{1+\epsilon^2} + C_1\omega + C_0$$

with $\epsilon = (\omega - \omega_0)/\Gamma$. Here, ω_0 is the position of the "naked" phonon, ω the Raman shift, Γ the width of the peak, q an asymmetry parameter, and I_0 a scaling factor. A background $(C_1\omega + C_0)$ that increases linearly in intensity with increasing Raman shift is assumed to take into account the observed shape of the phonon plus electronic background. The line shape reproduced the data well, as seen in Fig. 3. Within the precision of fitting the rather broad peak (± 2 cm^{-1}), $\omega_0 = 348$ cm^{-1} and there was no discernible variation of frequency with temperature. The peak narrows upon cooling with $\Gamma \approx 17$ cm^{-1} at RT and $\Gamma \approx 13$ cm^{-1} at 4 K. The asymmetry parameter q is about -1.3.

Figure 4 illustrates the Raman spectra of the nonsuper-

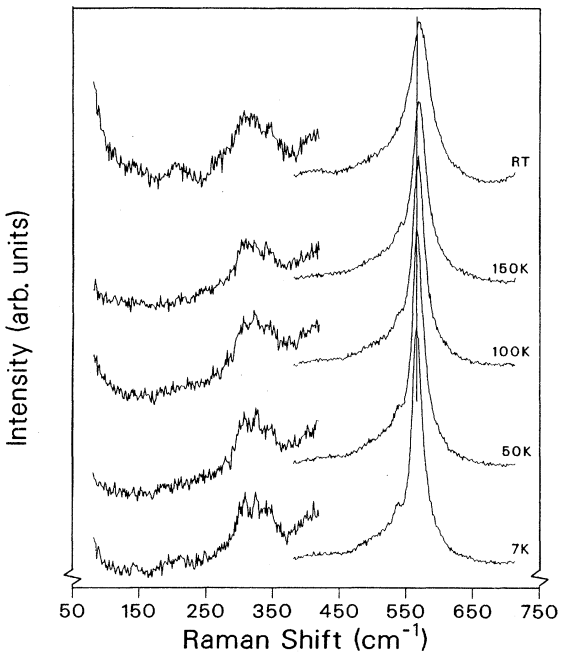

FIG. 4. Raman spectra of nonsuperconducting $Ba_{0.8}K_{0.2}BiO_3$ (high density) between RT and 7 K. Low-frequency regions are magnified by a factor of 4 compared to the high-frequency regions. Absolute scaling of low-frequency regions is the same as in Fig. 3. Spectra have linear offsets for clarity. Unlike superconducting $Ba_{0.6}K_{0.4}BiO_3$ (Fig. 3), the peak centered around 325 cm^{-1} does not exhibit the Fano line shape.

conducting phase $Ba_{0.8}K_{0.2}BiO_3$ (high density) between 295 and 7 K. Like superconducting $Ba_{1-x}K_xBiO_3$ (samples prepared with $x \geq 0.35$), $Ba_{0.8}K_{0.2}BiO_3$ has a broad peak centered around $\sim$325 cm^{-1}. $Ba_{0.8}K_{0.2}BiO_3$ has an intense, sharp peak at 569 cm^{-1} (RT value), similar to the intense peak found at the same frequency in monoclinic $BaBiO_3$,[12] Importantly, the peak centered around 325 cm^{-1} does not develop the Fano line shape upon cooling. That is, down to the lowest temperature measured, 7 K, the peak lacks the characteristic asymmetric shape and does not penetrate beneath the background on the high-frequency side. There are, however, other changes that occur upon cooling. The broad feature centered around 325 cm^{-1} develops reproducible structure, roughly splitting into a triplet. In addition, the intense peak found at 569 cm^{-1} at RT softens to 565 cm^{-1} at 7 K and develops a shoulder at $\sim$540 cm^{-1}.

The peaks in the Raman spectra of $Ba_{0.6}K_{0.4}BiO_3$ can be reasonably assigned to first-order phonon scattering that derives its intensity from disorder effects. To begin with, the lack of magnetic moments[3] precludes magnon scattering. With symmetries $3F_{1u}+F_{2u}$ at the Γ point of the Brillouin zone, the optical vibrational modes of the cubic perovskite $Ba_{1-x}K_xBiO_3$ are not Raman allowed in principle in first order. (The F_{1u} modes are Raman inactive and ir active while the "silent" F_{2u} mode is both ir and Raman inactive.) However, $Ba_{0.6}K_{0.4}BiO_3$ has inherent disorder arising from the substitution of K for Ba, in addition to other likely sources of disorder such as defects. These effects reduce the local and translational symmetry, allowing Raman scattering to occur from single phonons not necessarily at the Γ point. Indeed, the high-frequency Raman spectrum (>250 cm^{-1}) of $BaPb_{0.7}Bi_{0.3}O_3$ (Ref. 12) agrees well with the generalized one-phonon density of states of $BaPb_{0.75}Bi_{0.25}O_3$.[15] Disorder-induced, first-order scattering is found in other cubic perovskites[16] and in substitutional compounds with the NaCl structure, another structure for which first-order scattering is not strictly allowed.[17]

The 348-cm^{-1} peak of $Ba_{0.6}K_{0.4}BiO_3$ cannot arise from first- or second-ordering scattering from acoustic phonons since the acoustic phonons in oxide perovskites, including $BaPb_{0.75}Bi_{0.25}O_3$, all occur below $\sim$140 cm^{-1}.[18,19] Therefore, the peak must result from an optical phonon. The temperature dependence of the intensity is also supportive of first-order scattering. The peak at 348 cm^{-1} is twice as intense at 4 K as at RT. While both first- and second-order scattering should decrease in intensity, the observed increase is more consistent with first-order scattering since second-order scattering should diminish in intensity significantly more than first-order scattering upon cooling. Finally, given the high frequency of 348 cm^{-1}, the phonon must be dominated by O vibration.

Compared to cubic $Ba_{1-x}K_xBiO_3$, noncubic $Ba_{1-x}K_xBiO_3$ ($0 \leq x < 0.375$) has increased scattering intensity above 375 cm^{-1} (Fig. 2). The greater intensity arises from vibrational modes that become Raman allowed due to distortions of the BiO_6 octahedra and a larger unit cell. For example, the orthorhombic (*Immm*) structure of $Ba_{0.96}K_{0.04}BiO_3$ (Ref. 10) has $4A_g+2B_{1g}+3B_{2g}+3B_{3g}+A_u+4B_{1u}+5B_{2u}+5B_{3u}$ optical modes at the Γ point, with the g modes being Raman allowed and all the u modes except A_u being ir allowed. While it is not known whether all the noncubic phases have this exact supercell structure, similar normal-mode symmetries should be found for closely related supercell structures. The principal difference between $Ba_{0.8}K_{0.2}BiO_3$ and $Ba_{0.6}K_{0.4}BiO_3$ is the intense peak at 569 cm^{-1} in $Ba_{0.8}K_{0.2}BiO_3$. Here, as for $BaBiO_3$ (Ref. 12), the 569-cm^{-1} peak is assigned to the "breathing" mode of the BiO_6 octahedra. This mode is Raman-allowed in orthorhombic (*Immm*) $Ba_{1-x}K_xBiO_3$ (A_g) and monoclinic $BaBiO_3$ (A_g) but not in cubic $Ba_{1-x}K_xBiO_3$. Since the intensity of the peak centered around 325 cm^{-1} is essentially the same in cubic and noncubic $Ba_{1-x}K_xBiO_3$, it is likely that the $\sim$325-cm^{-1} peak of the noncubic phase derives its Raman intensity from disorder effects, as in the cubic phase.

Neutron-scattering intensity has been observed in $BaPb_{0.75}Bi_{0.25}O_3$, a superconducting phase closely related to $Ba_{0.6}K_{0.4}BiO_3$, at $\sim$340 cm^{-1} (42 meV).[15,19] Reichardt and co-workers analyzed tetragonal $BaPb_{0.75}Bi_{0.25}O_3$ in terms of the cubic perovskite and found the Γ-point frequencies of the TO phonons at about 104, 192, 196, and 527 cm^{-1}, apparently accounting for the $3F_{1u}+F_{2u}$ optical modes.[15,19] This investigation could not detect the expected LO branch of "breathing-type" vibrations of the O octahedra. Instead, scattering intensity was found at $\sim$340 cm^{-1} in a longitudinal geometry for phonon wave vectors away from the Γ point. The inability in the neu-

tron measurements of $BaPb_{0.75}Bi_{0.25}O_3$ to trace the 340-cm^{-1} feature toward the Γ point led to the conclusion that the feature was a local mode associated with a high-density lattice defect.[15] Further, it was proposed that the defects were static breathing-type distortions of O octahedra and the local phonon modes were the breathing-type vibrations of the distorted O octahedra. Undoubtedly, the $\sim$340-cm^{-1} phonon has the same origin as the peak centered around 325 cm^{-1} in the Raman spectra of $Ba_{1-x}K_xBiO_3$, $0.2 \leq x \leq 0.4$. Further, Sugai *et al.*[12] found Raman peaks at nearly the same frequency for $BaPb_{1-x}Bi_xO_3$ and the frequency and intensity were relatively independent of x between the limits studied, 0.17 to 1.0.

While the present investigation cannot assign the $\sim$325-cm^{-1} phonon of the Bi-based perovskites, several comments are in order. First, the Raman frequency is insensitive to doping on either the Ba sites ($Ba_{1-x}K_xBiO_3$) or the Bi sites [$BaPb_{1-x}Bi_xO_3$ (Ref. 12)]. Second, within either the K-doped system or the Pb-doped system,[12] the Raman intensity is relatively insensitive to the level of doping. Concerning the distorted O octahedra invoked to explain the 340-cm^{-1} mode of $BaPb_{0.75}Bi_{0.25}O_3$,[15] it seems unlikely that their density and extent of distortion would be insensitive to the type and extent of doping. Moreover, in cubic $Ba_{1-x}K_xBiO_3$, there is no structural evidence for distorted O octahedra. Instead, it is suggested that optical modes not involving full octahedral coordination be considered for the phonon. The layered Cu-based superconductors have Cu coordinated by O in square pyramids and square planes[1] while in $Nd_{2-x}Ce_xCuO_4$, Cu is coordinated only in square planes.[20] The optical modes of a square plane include, however, a normal mode of O vibration analogous to the silent mode of cubic perovskite.

There are similarities between the electron-phonon coupling observed in the cubic perovskite $Ba_{0.6}K_{0.4}BiO_3$ and the highly anisotropic triple perovskite $YBa_2Cu_3O_7$ ($T_c \approx 90$ K). The latter material has a phonon at 340 cm^{-1} that is coupled to electronic states as evidenced by the Fano line shape and anomalous frequency dependence upon entering the superconducting state by changes in temperature[6] or magnetic field.[14] The 340-cm^{-1} phonon (B_{1g} symmetry, assuming a tetragonal unit cell) is derived from the silent mode of cubic perovskite and consists of vibration along the c axis of the O atoms that form a square plane around the Cu atoms of the Cu-O planes.[21] The O atoms at adjacent corners of the square plane move in opposite directions. The B_{1g} mode is found around 300 cm^{-1} in other Cu-based superconducting phases: 278 cm^{-1} in $TlCaBa_2Cu_2O_7$ (Ref. 11), and 282 cm^{-1} in $Bi_2CaSr_2Cu_2O_8$.[22] While the silent F_{2u} mode is found around $\sim$300 cm^{-1} in many oxide perovskites,[18,23] it occurs at $\sim$196 cm^{-1} in $BaPb_{0.75}Bi_{0.25}O_3$.[15]

In this research, we have shown that an optical phonon at 348 cm^{-1} (43 meV) is coupled to electronic states in superconducting $Ba_{0.6}K_{0.4}BiO_3$. There are at least two ways of considering this experimental finding. Alternative possibilities to a conventional, phonon-mediated mechanism include *mechanisms mediated by predominantly electronic excitations.* Our experimental results are consistent with the hypothesis that the observed electron-phonon coupling is a consequence of "parasitic" phonon involvement in a mechanism mediated by electronic excitations.[3] On the basis of experimental measurements, including determinations of the energy gap,[24,25] $Ba_{0.6}K_{0.4}BiO_3$ and $BaPb_{0.75}Bi_{0.25}O_3$ are hypothesized to be in the weak-coupling limit, i.e., $\lambda < 1$.[3,24,25] If the weak-coupling mechanism in these relatively high-T_c compounds is predominantly phonon mediated, then coupling to high-frequency phonons is required. The Raman-scattering results reported here have identified such a high-frequency optical phonon in the system $Ba_{1-x}K_xBiO_3$.

The authors thank R. F. Wertenberg for performing the curve fitting of the Raman spectra and acknowledge support by the U.S. Department of Energy, Office of Basic Energy Sciences, Division of Material Sciences under Contracts No. DEAC04-76DP00789 (Sandia) and No. W-31-109-ENG-38 (Argonne). Work at Lawrence Livermore National Laboratory and University of California–Davis was performed under the auspices of the U.S. Department of Energy under Contract No. W-7405-ENG-48.

[1] A. W Sleight, Science **242**, 1519 (1988).
[2] R. J. Cava *et al.*, Nature (London) **332**, 814 (1988).
[3] B. Batlogg *et al.*, Phys. Rev. Lett. **61**, 1670 (1988).
[4] L. F. Mattheiss and D. R. Hamann, Phys. Rev. Lett. **60**, 2681 (1988); Phys. Rev. B **28**, 4227 (1983).
[5] T. M. Rice and L. Sneddon, Phys. Rev. Lett. **47**, 689 (1981).
[6] S. L. Cooper *et al.*, Phys. Rev. B **37**, 5920 (1988).
[7] D. G. Hinks *et al.*, Physica C **156**, 477 (1988).
[8] D. G. Hinks *et al.*, Appl. Phys. Lett. **54**, 1585 (1989).
[9] D. G. Hinks *et al.*, Nature (London) **333**, 836 (1988).
[10] L. F. Schneemeyer *et al.*, Nature (London) **335**, 421 (1988).
[11] K. F. McCarty *et al.*, Physica C **156**, 119 (1988).
[12] S. Sugai *et al.*, Phys. Rev. Lett. **55**, 426 (1985).
[13] M. V. Klein, in *Light Scattering in Solids I*, edited by M. Cardona, Topics in Applied Physics, Vol. 8 (Springer-Verlag, New York, 1975), p. 169.
[14] T. Ruf, C. Thomsen, R. Liu, and M. Cardona, Phys. Rev. B **38**, 11985 (1988).
[15] W. Reichardt and W. Weber, Jpn. J. Appl. Phys. **26**, Suppl. 3, 1121 (1987).
[16] G. A. Barbosa and J. I. Dos Santos, J. Raman Spectrosc. **10**, 100 (1981).
[17] G. Güntherodt, A. Jayaraman, W. Kress, and H. Bilz, Phys. Lett. **82A**, 26 (1981).
[18] R. A. Cowley, Phys. Rev. **134**, A981 (1964).
[19] W. Reichardt, B. Batlogg, and J. P. Remeika, Physica B **135**, 510 (1985).
[20] Y. Tokura, H. Takagi, and S. Uchida, Nature (London) **337**, 345 (1989).
[21] R. Liu *et al.*, Phys. Rev. B **37**, 7971 (1988).
[22] G. Burns *et al.*, Phys. Rev. B **39**, 2245 (1989).
[23] G. Burns, Phys. Rev. B **10**, 1951 (1974).
[24] Z. Schlesinger, R. T. Collins, B. A. Scott, and J. A. Calise, Phys. Rev. B **38**, 9284 (1988).
[25] Z. Schlesinger *et al.* (unpublished).